European Journal of Pharmacology 982 (2024) 176949



Contents lists available at ScienceDirect

European Journal of Pharmacology

journal homepage: www.elsevier.com/locate/ejphar

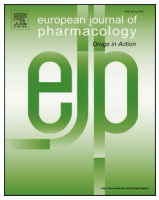



"Investigation of the potential cellular changes induced by magnesium sulfate and salubrinal in a lipopolysaccharide-induced chorioamnionitis model"

Halil Asci [a], Mehtap Savran [a], Muhammet Y. Tepebasi [b], Ilter Ilhan [c], Nasif F. Karakuyu [d], Orhan B. Imeci [a,*], Mehmet A. Sevuk [a], Mekin Sezik [e], Ozlem Ozmen [f]

[a] Suleyman Demirel University, Faculty of Medicine, Department of Pharmacology, Isparta, Turkey
[b] Suleyman Demirel University, Faculty of Medicine, Department of Medical Genetic, Isparta, Turkey
[c] Suleyman Demirel University, Faculty of Medicine, Department of Biochemistry, Isparta, Turkey
[d] Suleyman Demirel University, Faculty of Pharmacy, Department of Pharmacology, Isparta, Turkey
[e] Suleyman Demirel University, Faculty of Medicine, Department of Obstetrics and Gynecology, Isparta, Turkey
[f] Burdur Mehmet Akif Ersoy University, Faculty of Veterinary, Department of Pathology, Burdur, Turkey

ARTICLE INFO

Keywords:
Chorioamnionitis
Lipopolysaccharides
Salubrinal
Endoplasmic reticulum
Apoptosis

ABSTRACT

Chorioamnionitis is closely associated with preterm labor and poses a significant public health concern. In this pathological process where inflammation plays a key role, intracellular mechanisms such as endoplasmic reticulum stress are crucial. In this study, we aimed to explore the potential positive outcomes of the combined use of salubrinal (SLB) with magnesium (Mg) treatment in chorioamnionitis.

Thirty pregnant rats were divided into 5 groups as: Control, LPS (1 mg/kg), LPS + SLB (1 mg/kg), LPS + Mg (Dhaka protocol), LPS + SLB + Mg. Rats were sacrificed 4 h after LPS administration, then placental and fetal brain tissues were collected.

LPS administration enhanced the levels of tumor necrosis factor-alpha, vascular endothelial growth factor, caspase-3 immunoexpressions, BAX, eukaryotic initiation factor 2-alpha, s100, and glial fibrillary acidic protein expressions and lowered BCL2 expressions in the placenta or fetal brains. SLB and Mg treatments were observed to reverse all these findings, and the most significant positive effect was in the LPS + SLB + Mg group.

The known anti-inflammatory activity of Mg, when used with SLB, preventing the transition to apoptosis and increasing antioxidant enzyme activity, as identified in this study, can contribute significantly to the literature. However, these results need to be supported by additional molecular studies.

1. Introduction

Chorioamnionitis is an inflammatory condition that may arise due to premature birth, membrane rupture, prolonged labor, tobacco use, and infection (Ohyama et al., 2002). Studies indicate that placental or chorionic membrane infections can be significant contributors to preterm births (Conti et al., 2015; Perkins et al., 1988). Infections are commonly of bacterial origin, posing risks for the mother and the fetus. Among the newborn complications associated with chorioamnionitis are premature birth, cerebral palsy, neurological abnormalities, and sepsis, with some cases progressing to a potentially fatal course (Heine et al., 2017).

Perinatal brain injury (PBI) can lead to long-term neurodevelopmental disorders, affecting cognition, neurology, motor skills, and sensory functions. Infants born before the 32nd week of pregnancy are more susceptible to PBI compared to full-term infants (Larroque et al., 2008). The fundamental mechanism of this damage involves hypoxic-ischemic or inflammatory processes triggering a series of events that exacerbate PBI. Preterm fetuses, lacking a mature cerebrovascular autoregulation system, struggle to adapt physiologically, leading to heightened cellular damage in response to proinflammatory cytokines such as tumor necrosis factor-alpha (TNF-α), vascular endothelial growth factor (VEGF), and reactive oxygen species (ROS) produced in hypoxic-ischemic situations (Eklind et al., 2001; Novak et al., 2018). Among the mechanisms of developing cellular damage, endoplasmic reticulum (ER) stress plays a crucial role.

Proteins must undergo posttranslational modifications in the ER to

* Corresponding author.
E-mail address: orhanimeci@sdu.edu.tr (O.B. Imeci).

https://doi.org/10.1016/j.ejphar.2024.176949
Received 18 April 2024; Received in revised form 23 August 2024; Accepted 26 August 2024
Available online 27 August 2024
0014-2999/© 2024 Elsevier B.V. All rights are reserved, including those for text and data mining, AI training, and similar technologies.

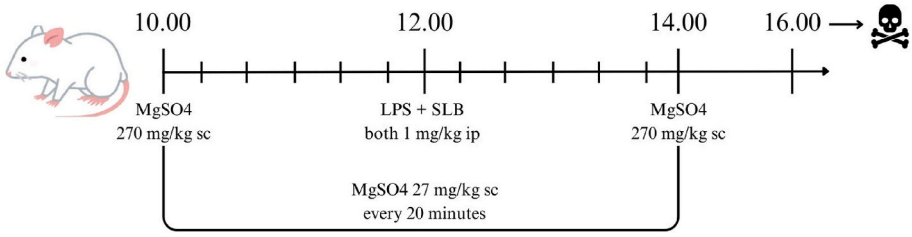

Fig. 1. Experimental design.

Table 1
Primary sequences, product size and accession numbers of genes.

Genes	Primary sequence	product size	accession number
GAPDH (HouseKeeping)	F: AGTGCCAGCCTCGTCTCATA R: GATGGTGATGGGTTTCCCGT	248 bp	NM_017008.4
Rn18s (HouseKeeping)	F: CTCTAGATAACCTCGGGCCG R: GTCGGGAGTGGGTAATTTGC	209 bp	NR_046237.2
BAX	F: AGGGTGGCTGGGAAGGC R: TGAGCGAGGCGGTGAGG	93 bp	XM_039087751.1
BCL2	F: ATCGCTCTGTGGATGACTGAGTAC R: AGAGACAGCCAGGAGAAATCAAA	134 bp	NM_016993.2
eIF2α	F: GGTTACGAAGGCATTGATGCTG R: TGTCATCACATACCTGGGTGGAG	114 bp	NM_019356.1
s100	F: GGGAATCACCATGCCCTCTA R: CCCACCCTTATCACCAACACA	167 bp	XM_006232565.4
GFAP	F: AAATTGCTGGAGGGCGAAGA R: GGGCACACCTCACATCACAT	207 bp	NM_017009.2

F: Forward, R: Reverse, GAPDH: Glyceraldehyde-3-phosphate dehydrogenase, Rn18s: 18S ribosomal RNA, BAX: BCL2 Associated X, BCL2: B-cell lymphoma 2, eIF2α: Eukaryotic translation initiation factor 2 subunit alpha, s100: S100 calcium binding protein, GFAP: glial fibrillary acidic protein.

perform their functions (Oakes and Papa, 2015). However, pathological events such as infection, hypoxia, and redox imbalances disrupt ER homeostasis, accumulating misfolded proteins in the ER lumen and causing ER stress (Ron and Walter, 2007; Zhang and Kaufman, 2004). Additionally, ROS-related mitochondrial stress can combine with ER stress to induce apoptosis. Given these mechanisms, chorioamnionitis-associated PBI is a multifaceted pathology requiring molecules that target key cellular points for effective treatment.

Salubrinal (SLB) selectively inhibits the dephosphorylation of eukaryotic initiation factor 2 alpha (eIF2α), reducing protein synthesis and alleviating ER workload to provide cytoprotective effects (Matsuoka and Komoike, 2015). Studies have reported SLB's ability to prevent ER-mediated apoptosis, neuroinflammation, and ROS production, reducing oxidative stress (Deselms et al., 2016; Roth et al., 2014; Rubovitch et al., 2015). It has also been shown to inhibit the mitochondrial apoptotic pathway and decrease inflammatory cytokines like TNF-α and microglial activation (Bracchi-Ricard et al., 2013; Huang et al., 2012; Tan et al., 2018).

Magnesium sulfate (MgSO4) has proven to protect placental and fetal tissues by inhibiting intracellular mechanisms central to the nuclear factor kappa-beta pathway, reducing inflammation (Khatib et al., 2020). Magnesium (Mg), an N-methyl-D-aspartate (NMDA) receptor antagonist, emerges as a significant protective agent, especially in excitotoxicity-induced neuronal damage.

Considering the above information, this study aims to investigate the potential positive changes induced at the cellular level by MgSO4 and SLB separately and in combination in a lipopolysaccharide (LPS)-induced preterm labor with chorioamnionitis model.

2. Materials and methods

2.1. Experimental animals

In the experimental model, adult female Wistar Albino rats aged 10–14 weeks and weighing between 250 and 300 g were utilized. The rats were kept under conditions of 22–24 °C with a 12-h light and 12-h dark cycle. They were provided ad libitum feeding. Euro type 4 cages were used for housing the rats. Procedures have been carried out considering the guidelines for Animal Research: Reporting in Vivo Experiments (ARRIVE) 2.0 at all stages of the experiment. The experimental protocol was approved by the Animal Experiments Ethics Committee of Suleyman Demirel University with the number: March 17, 2022/08–42.

It is known that the normal gestation period in rats, under standard conditions (term), is approximately 21–23 days following mating. In this study, male and female rats were housed together in the same cage, and vaginal smear samples were collected daily starting one day after cohabitation. The day on which sperm cells were detected under the microscope was considered as day 1 of pregnancy, and experimental preterm birth was induced by controlled cesarean section (hysterotomy) on the 17th day. Randomization was conducted on the 10th day of pregnancy. This study has been supported by the Scientific Research Projects Coordination Unit of Suleyman Demirel University under project number TYL-2019-7406 and by Scientific and Technological Research Council of Türkiye under project number 222S711.

2.2. Experimental procedure

Pregnant rats were divided into 5 groups. Experimental groups were created with 6 animals in each group as follows:

Control group: On the 17th day of pregnancy, a loading dose of physiological saline (0.5–1 ml volume) was administered subcutaneously (sc) at 0 and 4 h, followed by maintenance doses of physiological saline (0.5–1 ml volume) every 20 min, totaling 10 applications. At the 2nd hour, physiological saline (0.5–1 ml volume) was administered intraperitoneally (ip). Simultaneously, physiological saline (0.5–1 ml volume) was administered ip in the right inguinal region.

LPS group: On the 17th day of pregnancy, a loading dose of physiological saline was administered sc at 0 and 4 h, followed by maintenance doses of physiological saline every 20 min, totaling 10 applications. At

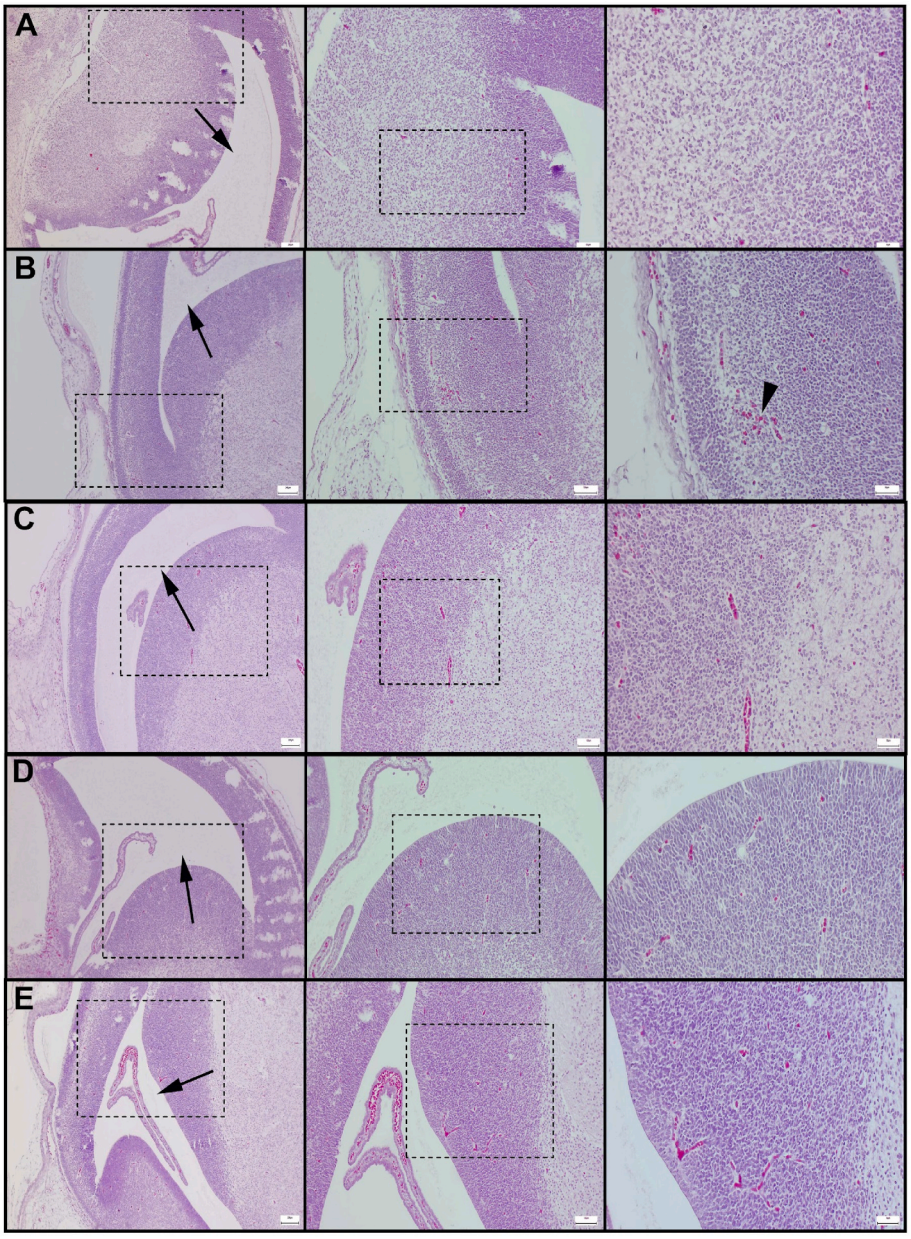

Fig. 2. Histopathological appearance of the cerebral cortex of rat brains
Normal microscopic view of a fetal rat cerebral cortex and ventricle (arrow) in the control group (A), Microhemorrhage areas (arrowhead) in LPS group (B), Hyperemia in the brain tissue of LPS + SLB group (C), Mild hyperemia in a fetal cerebral cortex and ventricle (arrow) in the LPS + Mg group (D), Very mild hyperemia in LPS + SLB + Mg group (E); Dashed areas: Areas selected for magnification on the right, HE, Bars 200 μm, 100 μm and 50 μm, respectively.

the 2 nd h, LPS (1 mg/kg) was administered ip. Simultaneously, physiological saline was administered ip in the right inguinal region (Yavuz et al., 2017).

LPS + SLB group: On the 17th day of pregnancy, a loading dose of physiological saline was administered sc at 0 and 4 h, followed by maintenance doses of physiological saline every 20 min, totaling 10 applications. At the 2nd hour, LPS was administered ip. Simultaneously, SLB (1 mg/kg) was administered ip in the right inguinal region (Wang et al., 2019).

LPS + Mg group: On the 17th day of pregnancy, a loading dose of MgSO4 (270 mg/kg) was administered sc at 0 and 4 h, followed by maintenance doses of MgSO4 (27 mg/kg) every 20 min, totaling 10 applications (Beloosesky et al., 2016). At the 2nd hour, LPS was administered ip (fingolimod). Simultaneously, physiological saline was administered ip in the right inguinal region.

LPS + SLB + Mg group: On the 17th day of pregnancy, a loading dose of MgSO4 (270 mg/kg) was administered sc at 0 and 4 h, followed by maintenance doses of MgSO4 (27 mg/kg) every 20 min, totaling 10 applications. At the 2nd hour, LPS (1 mg/kg) was administered ip. Simultaneously, SLB (1 mg/kg) was administered ip in the right inguinal region. Experimental design was shown in Fig. 1.

The experimental group shown in the figure is the LPS + SLB + Mg group. In the other groups, saline of the same volume was used as a control for all three substances. LPS: Lipopolysaccharide, SLB: Salubrinal, MgSO4: Magnesium sulfate.

Four hours after the LPS application, all rats in the groups were sacrificed under Ketamine (90 mg/kg, Keta-Control, Doğa İlaç, Turkey) and Xylazine (10 mg/kg, Xylazinbio, Bioveta, Czech Republic) anesthesia. Euthanasia was performed through surgical exsanguination by collecting blood from the inferior vena cava following abdominal

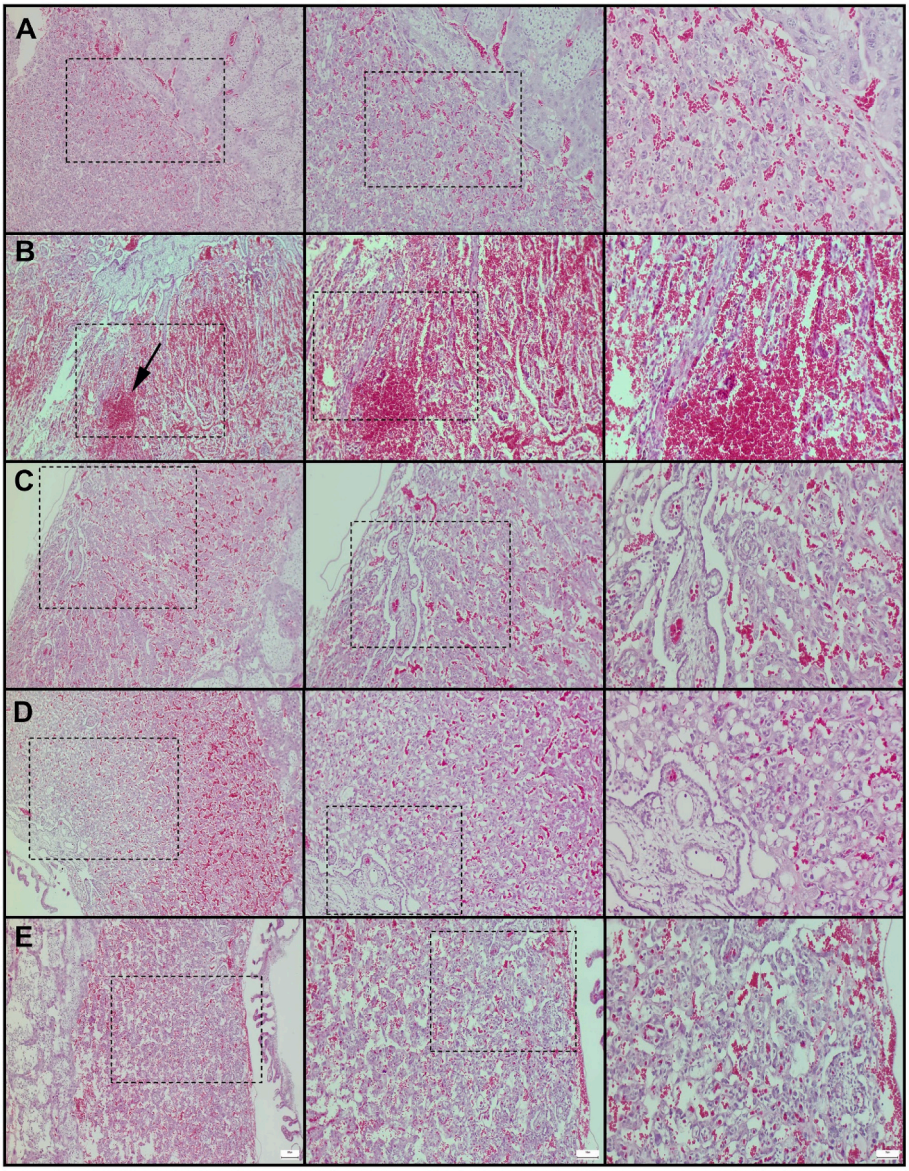

Fig. 3. Histopathological appearance of the placentas of rats.

incision. One fetal brain and placental tissue samples from each mother were collected and put into 10% formaldehyde solution for histopathological, −80 for biochemical and genetic analysis.

2.3. Histopathological analysis

During necropsy, placental and fetal brain samples taken from rats were fixed in 10% neutral formaldehyde solution. The tissues, kept in formaldehyde for two days, were longitudinally trimmed and placed on tissue processing cassettes and placed in a fully automatic tissue processor (Leica ASP300S; Leica Microsystem, Nussloch, Germany) for routine histological processing. The tissues were embedded in paraffin and 5 μm thickness sections were obtained using a Leica 2155 rotary microtome (Leica Microsystem, Nussloch, Germany). The sections stained with hematoxylin and eosin (HE). Subsequently, cleared in xylene and coverslipped. After drying for a day, the sections were ready for examination under an Olympus CX21 model light microscope. The examined preparations were digitally photographed using an Olympus DP26 model camera and transferred to a computer.

2.4. Immunohistochemical analysis

Sections obtained from paraffin blocks were immunohistochemically stained according to the manufacturer's protocol for Caspase-3 (Cas-3) (anti-caspase-3 antibody (E−8): sc-7272), VEGF (VEGF (JH1212: sc-57496, 1/100 dilution; Santa Cruz, Texas, USA), and TNF-α (Anti-TNF-α antibody [52B83]: sc-52746, 1/100 dilution; Santa Cruz, Texas, USA) by the streptavidin–biotin technique following the manufacturer's instructions. The sections were incubated with primary antibodies for 60 min. Immunohistochemistry was then performed using biotinylated secondary antibody and streptavidin-alkaline phosphatase conjugate. Ready to use rabbit specific HRP/DAB Detection IHC Detection Kit - Micro-polymer (ab236469) (Abcam Cambridge, UK) was used as a secondary antibody and diaminobenzidine (DAB) as a chromogen (DAB Substrate Kit (ab64238), (Abcam, Cambridge, UK). Sections were incubated with DAB for 3–5 min. Antigen dilution solution was used instead of primary antibody for negative controls. All examinations were performed on blind specimens by a specialist pathologist from another university. Sections were separately investigated for each antibody for immunohistochemical analysis.

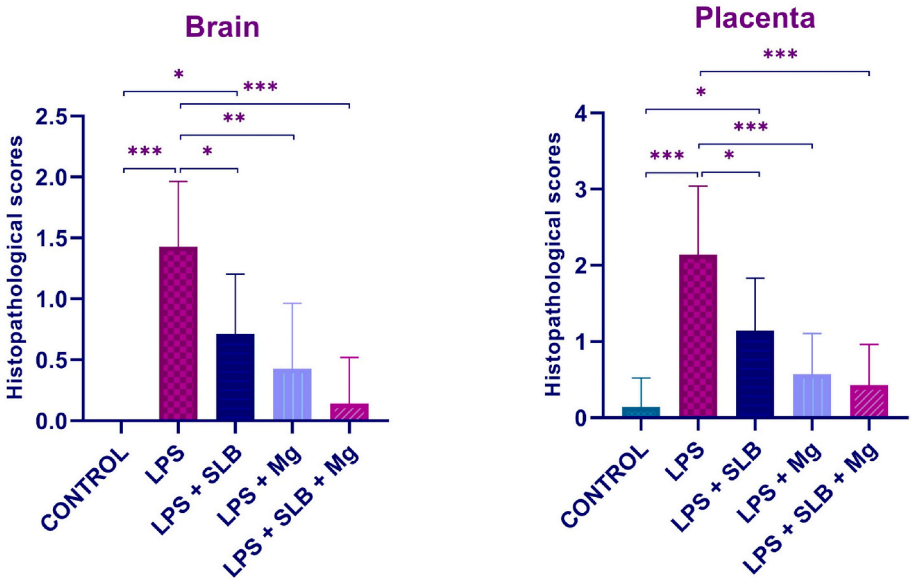

Fig. 4. Statistical results of histopathological findings
LPS: Lipopolysaccharide, SLB: Salubrinal, Mg: Magnesium. "*" denotes comparisons indicating statistical significance compared to the control group, with * $p < 0.05$, ** $p < 0.01$, and *** $p < 0.001$.

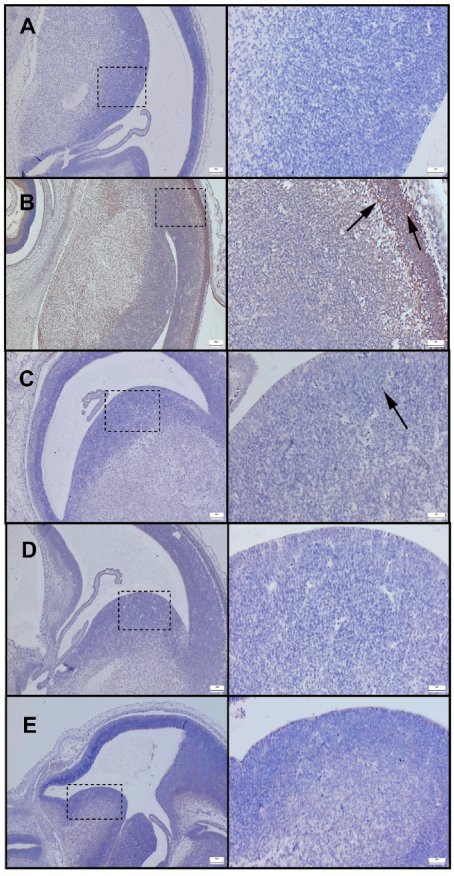

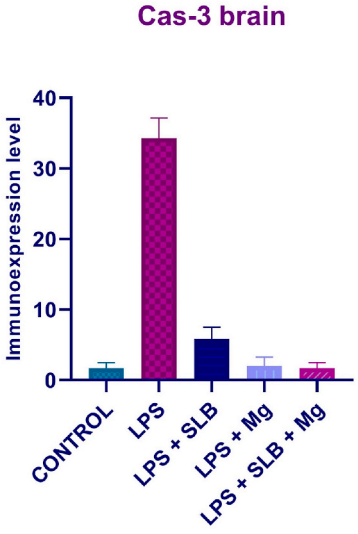

Posthoc LSD test	Summary	Individual P Value
CONTROL vs. LPS	***	<,001
CONTROL vs. LPS + SLB	***	<,001
CONTROL vs. LPS + Mg	ns	,750
CONTROL vs. LPS + SLB + Mg	ns	>,999
LPS vs. LPS + SLB	***	<,001
LPS vs. LPS + Mg	***	<,001
LPS vs. LPS + SLB + Mg	***	<,001
LPS + SLB vs. LPS + Mg	***	<,001
LPS + SLB vs. LPS + SLB + Mg	***	<,001
LPS + Mg vs. LPS + SLB + Mg	ns	,750

Fig. 5. Cas-3 immunoexpressions of fetal brain tissues
Negative Cas-3 expressions in a fetal brain in the control group (A), Severe Cas-3 expressions (arrows) in the brain of a fetal rat in the LPS group (B), Significantly decreased and sporadic cell expressions in the brain of a fetal rat in the LPS + SLB group (arrows) (C), Negative caspase expressions in the LPS + Mg group (D), Negative Cas-3 expression in the cerebral cortex in the LPS + SLB + Mg group (E). Streptavidin biotin peroxidase method, Bars 200 μm and 50 μm, respectively. LPS: Lipopolysaccharide, SLB: Salubrinal, Mg: Magnesium. *$p < 0.05$, **$p < 0.01$, and ***$p < 0.001$.

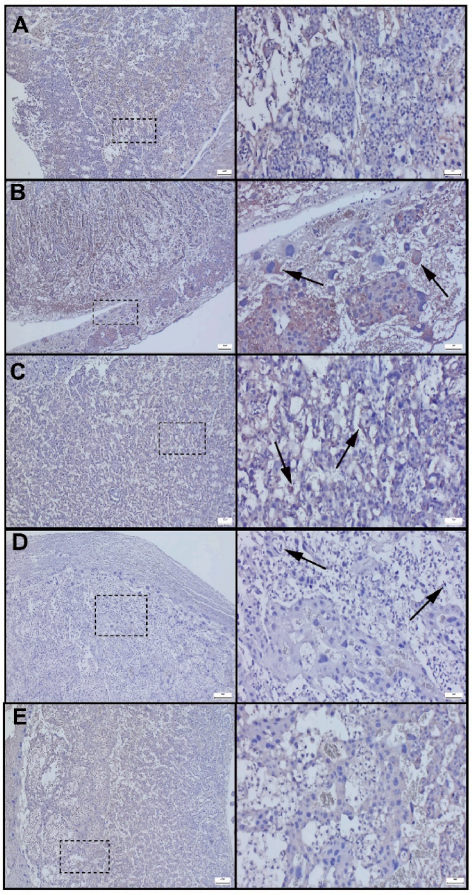

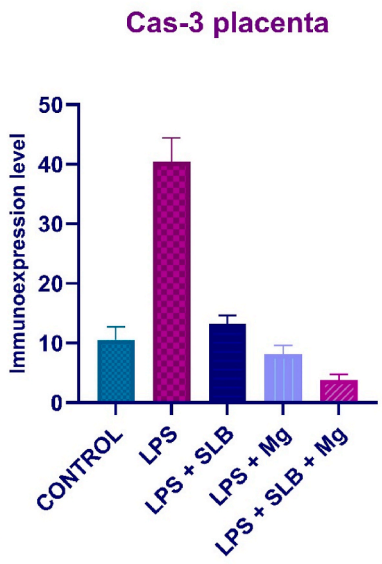

Tukey's multiple comparisons test	Summary	P Value
CONTROL vs. LPS	***	<,001
CONTROL vs. LPS + SLB	ns	,184
CONTROL vs. LPS + Mg	ns	,278
CONTROL vs. LPS + SLB + Mg	***	<,001
LPS vs. LPS + SLB	***	<,001
LPS vs. LPS + Mg	***	<,001
LPS vs. LPS + SLB + Mg	***	<,001
LPS + SLB vs. LPS + Mg	**	,001
LPS + SLB vs. LPS + SLB + Mg	***	<,001
LPS + Mg vs. LPS + SLB + Mg	**	,010

Fig. 6. Cas-3 immunoexpressions of placental tissues
Very mild placental immunoexpression in the control group (A), Significantly increased expressions in the LPS group (arrows) (B), Mild expressions (arrows) in the LPS + SLB group (C), Mild expressions (arrows) in the LPS + Mg group (D), Significantly decreased expressions in the LPS + SLB + Mg group (E), Streptavidin biotin peroxidase method, Bars 200 μm and 50 μm respectively. LPS: Lipopolysaccharide, SLB: Salubrinal, Mg: Magnesium. *p < 0.05, **p < 0.01, and ***p < 0.001.

To find the percentage of positive cells for each marker in each location, 100 cells from each group were counted at a magnification of × 40. The ImageJ program (version 1.48, National Institutes of Health, Bethesda, MD) was used to analyze the images. A statistical analysis was performed on the image analyzer's data. The Database Manual Cell Sens Life Science Imaging Software System (Olympus Co., Tokyo, Japan) was used for microphotography.

2.5. Biochemical analysis

Placental and brain tissues obtained for oxidative stress parameters were portioned, placed in Eppendorf tubes, and stored at −20 °C until the day of analysis. Then, tissues were diluted five-fold (w/v) with phosphate-buffered saline (10 mM sodium phosphate) at pH 7.4 and homogenized with a tissue homogenizer (IKA Ultra Turrax T25, Janke & Kunkel, Staufen, Germany). At the end of the homogenization, the samples were centrifuged at 2000 rpm/20 min/+4 °C (Nuve NF 1200R, Ankara, Turkey). Subsequently, they were transferred to the SDU Faculty of Medicine Biochemistry Laboratory for triple measurements. To assess oxidative stress, the levels of total antioxidant status (TAS) and total oxidant status (TOS) were analyzed using the spectrophotometric method based on Erel's protocol. TOS results were μmol H2O2 Equiv/g protein, and TAS results were mmol Trolox Equiv/g protein. The oxidative stress index (OSI) was calculated by dividing the TOS levels by TAS levels, that is, TOS/TASx100 (Özden et al., 2023).

2.6. Genetical analysis

Using the GeneAll RiboEx (TM) RNA Isolation Kit (Cat No: 301–001) and the manufacturer's instructions, RNA was extracted from homogenized placenta and fetal brain tissues (GeneAll Biotechnology, Seoul, Korea). A BioSpec-nano NanoDrop UV–Vis spectrophotometer (UV-2600, Shimadzu Ltd. Kyoto, Japan) instrument was used to measure the quantity and purity of the RNAs that were collected. cDNA synthesis was performed using the A.B.T.™ cDNA Synthesis Kit (Cat No: C03-01–05) from Atlas Biotechnology in Turkey according to the instructions. One microgram of RNA was used for cDNA synthesis. Using the Primer-BLAST tool, NCBI website, specific mRNA sequences were found, and potential primer sequences were then tested. In Table 1, the primers' sequences used, accession numbers, and product size of the genes are given. A.B.T.™ SYBR Master Mix (Atlas Biotechnology, Turkey) (Cat No: Q04-01–05) was used to quantify the expression levels of genes in a Biorad CFX96 real-time PCR equipment (CA, USA). In the research, the GAPDH gene was used as the housekeeping gene in the placenta tissue and the Rn18s gene was used as the housekeeping gene in the brain tissue. The reaction mixture was prepared according to the manufacturer's protocol to a final volume of 20 μL. The resultant reaction mixture was put into a real-time qPCR equipment with thermal cycling setup in accordance with the manufacturer's protocol for the kit, and each sample was examined in three replications. The PCR protocol was applied as 1 cycle with an initial denaturation at 95 °C for 300 s and 40 cycles with denaturation at 95 °C for 15 s, annealing/extension at 55 °C for 30 s. Relative mRNA levels were calculated by applying the $2^{-\Delta\Delta}$Ct formula to the normalize the results.

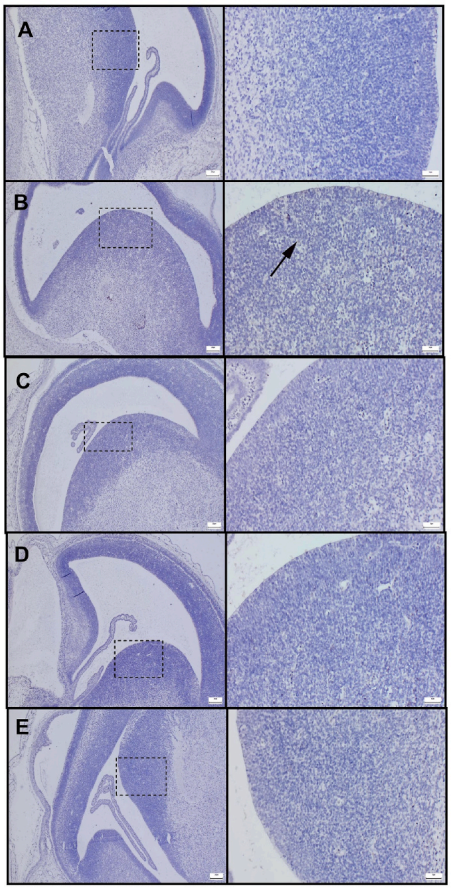

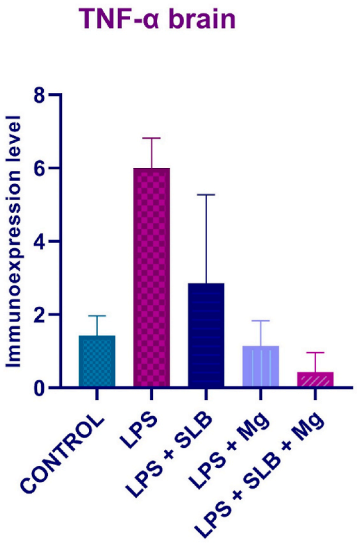

Posthoc LSD test	Summary	Individual P Value
CONTROL vs. LPS	***	<,001
CONTROL vs. LPS + SLB	*	,037
CONTROL vs. LPS + Mg	ns	,666
CONTROL vs. LPS + SLB + Mg	ns	,138
LPS vs. LPS + SLB	***	<,001
LPS vs. LPS + Mg	***	<,001
LPS vs. LPS + SLB + Mg	***	<,001
LPS + SLB vs. LPS + Mg	*	,014
LPS + SLB vs. LPS + SLB + Mg	***	<,001
LPS + Mg vs. LPS + SLB + Mg	ns	,285

Fig. 7. TNF-α immunoexpressions of fetal brain tissues
Negative TNF-α expression in a fetal rat brain in the control group (A), Very slight expression in the fetal rat in the LPS group (arrow) (B), Negative expression in the brain of a fetal rat in the LPS + SLB group (C), Negative expression in the brain of a fetal rat in the LPS + Mg group (D), Negative expression in the cerebral cortex of a rat in the LPS + SLB + Mg group (E), Streptavidin biotin peroxidase method, Bars 200 μm and 50 μm, respectively. LPS: Lipopolysaccharide, SLB: Salubrinal, Mg: Magnesium. *$p < 0.05$, **$p < 0.01$, and ***$p < 0.001$.

2.7. Statistical analysis

Due to the sample size being less than 30 in each group and the variance being unequal, a non-parametric statistical method was preferred in the evaluation of the data. The obtained data underwent logarithmic transformation, and for those not meeting the assumptions of parametric tests, non-parametric one-way ANOVA and post-hoc LSD tests were employed to determine differences among group rank means. Data meeting the assumptions of parametric tests were analyzed using factorial repeated measures analysis of variance. The presence of a linear relationship between all variables was examined by calculating Pearson correlation coefficients pairwise. The analysis results are presented as mean ± standard deviation, and $p < 0.05$ was considered statistically significant.

3. Results

3.1. Histopathology

In the histopathological examination of fetal brain samples collected during necropsy, the fetal brains in the control group appeared normal. In the fetal brains of the LPS group, severe hyperemia in the vessels, occasional microhemorrhages and mild inflammatory cell infiltration were observed. It was determined that SLB and Mg applications reduced pathological findings, while dual application had a more significant healing effect. During histopathological examination, care was taken to examine the cortex region of the fetal brains and, whenever possible, the same area (Fig. 2).

In the histopathological examination of the placenta samples, normal placenta histology was observed in the samples in the control group, while severe hyperemia, bleeding and occasional inflammatory cell infiltration were observed in the LPS group. It was noted that Mg and SLB applications significantly improved the lesions, and the improvement was much more evident in the double group (Fig. 3). The statistical analysis results of histopathological scores are shown in Fig. 4.

Normal appearance of the placenta of a rat in the control group (A), Severe hyperemia and significant hemorrhagic area (arrow) in the placenta of a rat in the LPS group (B), Mild hyperemia in the placenta in a rat in the LPS + SLB group (C), A near-normal appearance in the placenta of a rat in the LPS + Mg group (D), Normal placenta in a rat in the LPS + SLB + Mg group (E); Areas indicated by the dashed square are magnified at a higher scale on the right., HE, Bars 200 μm, 100 μm and 50 μm, respectively.

3.2. Immunohistochemistry

At the examination of the brain sections stained with Cas-3 immunohistochemistry, negative expression was noted in the control group. It was observed that Cas-3 expressions increased significantly in fetal brains in the LPS group. It was determined that SLB and Mg applications decreased the expressions. It was noted that Mg application was more effective in reducing Cas-3 expressions than SLB application. It was observed that double applications almost completely negated the expressions (Fig. 5).

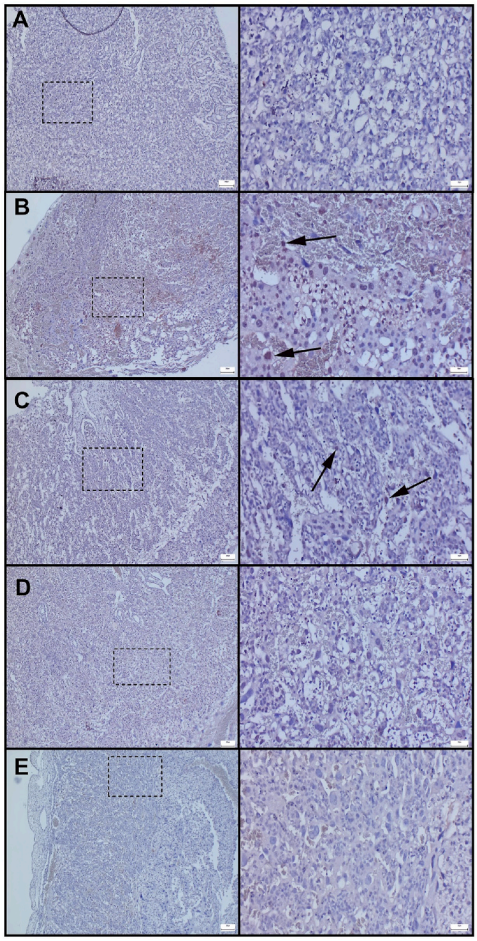

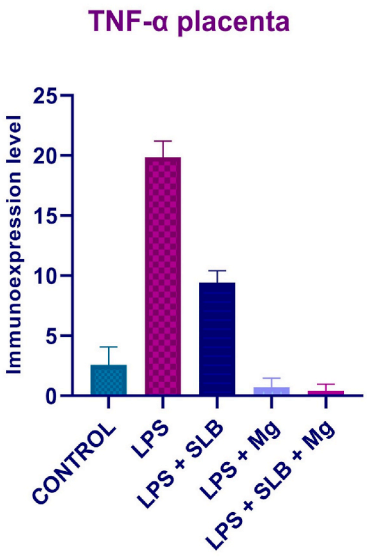

Posthoc LSD test	Summary	Individual P Value
CONTROL vs. LPS	***	<,001
CONTROL vs. LPS + SLB	***	<,001
CONTROL vs. LPS + Mg	**	,003
CONTROL vs. LPS + SLB + Mg	***	<,001
LPS vs. LPS + SLB	***	<,001
LPS vs. LPS + Mg	***	<,001
LPS vs. LPS + SLB + Mg	***	<,001
LPS + SLB vs. LPS + Mg	***	<,001
LPS + SLB vs. LPS + SLB + Mg	***	<,001
LPS + Mg vs. LPS + SLB + Mg	ns	,626

Fig. 8. TNF-α immunoexpressions of placental tissues
Negative TNF-α expressions in the placenta of a rat in the control group (A), Increased immunoreaction in the LPS group (arrows) (B), Very reduced and mild (arrows) immunoexpressions LPS + SLB group (C), Negative TNF-α expression in the LPS + Mg group (D), Negative TNF-α expression in the LPS + SLB + Mg group (E), Streptavidin biotin peroxidase method, Bars 200 μm and 50 μm, respectively. LPS: Lipopolysaccharide, SLB: Salubrinal, Mg: Magnesium. *$p < 0.05$, **$p < 0.01$, and ***$p < 0.001$.

When placental Cas-3 expressions were evaluated according to groups, it was noted that the expressions, which were very mild in the control group, increased significantly in the LPS group. It was observed that the expressions decreased in the SLB and Mg groups and decreased significantly in the dual applications (Fig. 6).

At the microscopic examination of brain sections, slight increases were detected in the LPS group, while negative expressions were noted in the other groups (Fig. 7). At the microscopic examination of TNF-α immunohistochemically stained placenta sections, negative expressions were observed in the control group, while expressions were significantly increased in the placentas of rats in the LPS group. It was noted that SLB and Mg applications reduced the expressions, while dual applications caused significant decreases in expressions (Fig. 8).

3.3. Biochemistry

The oxidative stress parameters were assessed in fetal brain and placental tissues. Significant increases in TOS and OSI values were observed in the fetal brain tissue when comparing the control and LPS groups ($p < 0.001$ and $p < 0.05$, respectively). When the LPS group was compared to the LPS + SLB group, significant decreases were noted in both TOS and OSI (both $p < 0.05$). The TAS levels in the LPS + SLB and LPS + SLB + Mg groups were significantly higher than those in the control group ($p < 0.05$ and $p < 0.01$, respectively). Additionally, OSI levels in the LPS + SLB + Mg group were significantly lower compared to the LPS group ($p < 0.05$).

In the examination of TOS levels in placental tissues, both LPS + Mg and LPS + SLB + Mg groups were found to be significantly lower than the LPS group (both $p < 0.01$). In the LPS group, placental OSI levels were significantly higher compared to the control, LPS + Mg, and LPS + SLB + Mg groups ($p < 0.05$, $p < 0.01$, $p < 0.05$, respectively) (Fig. 9).

3.4. Genetic

When examining gene expressions in fetal brain tissues, in the LPS group, BAX, eIF2α, s100, and GFAP levels were found to be significantly higher, while BCL2 level was significantly lower compared to the control group (all $p < 0.001$). In the LPS + SLB and LPS + Mg groups, BCL2 levels were significantly lower than the control group (both $p < 0.05$). In the LPS group, BAX, eIF2α, s100, and GFAP levels were significantly higher compared to the LPS + SLB, LPS + Mg, and LPS + SLB + Mg groups (s100, $p < 0.01$ for LPS + Mg, and $p < 0.001$ for all others). Conversely, BCL2 levels were significantly higher in the LPS + SLB, LPS + Mg, and LPS + SLB + Mg groups compared to the LPS group ($p < 0.01$, $p < 0.05$, and $p < 0.01$, respectively). Additionally, eIF2α and s100 levels in the LPS + Mg group were significantly higher compared to the LPS + SLB + Mg group (both $p < 0.05$) (Fig. 10).

When examining gene expressions in placental tissues, in the LPS group, BAX and eIF2α levels were significantly higher, while BCL2 level was significantly lower compared to the other four groups (all p <

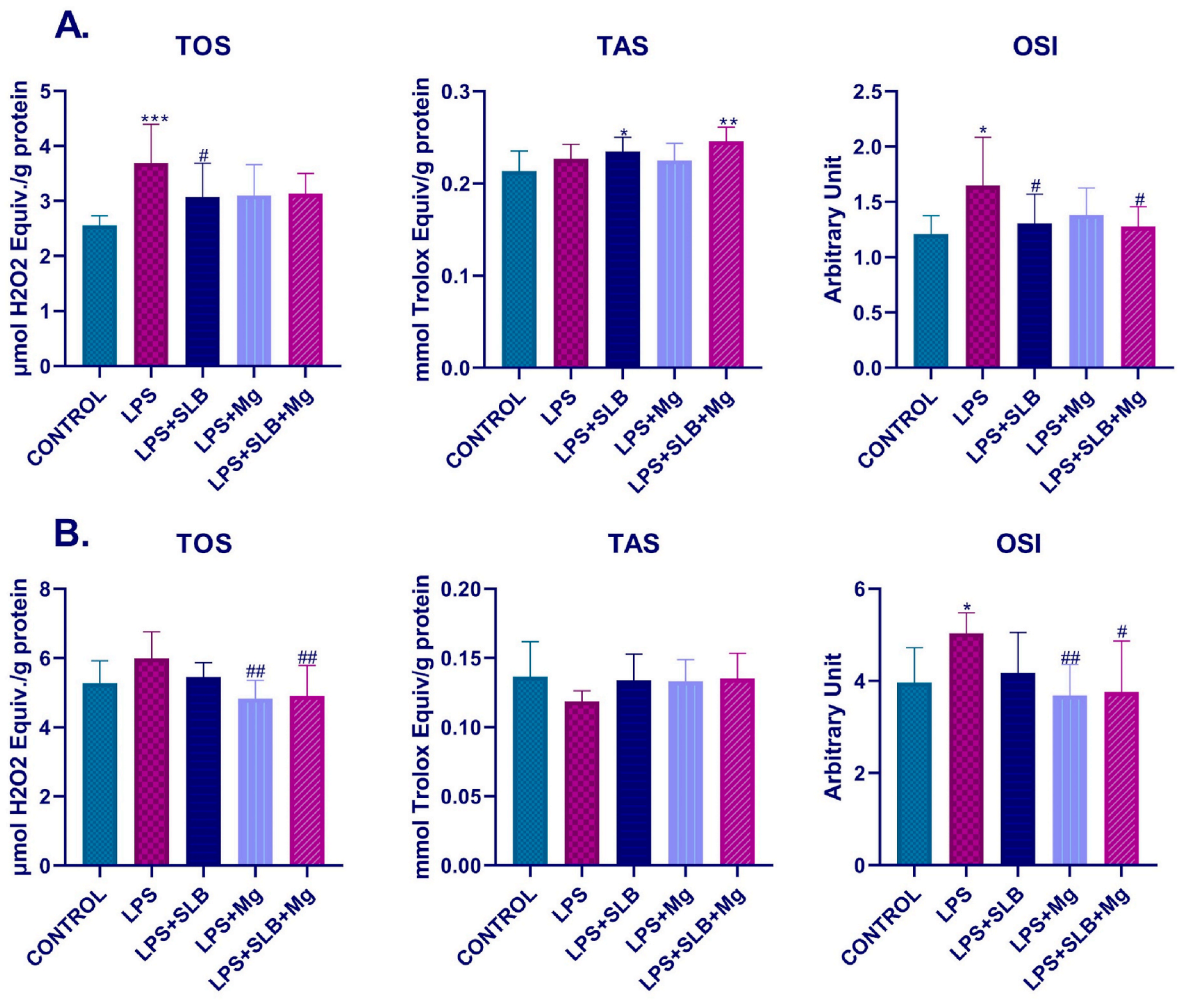

Fig. 9. The graphs of oxidative stress parameters in fetal brain and placental tissues
Data were expressed as mean ± standard deviation. A: Fetal Brain, B:Placenta, TOS: Total oxidant status, TAS: Total antioxidant status, OSI: Oxidative stress index, LPS: Lipopolysaccharide, SLB: Salubrinal, Mg: Magnesium. "*" denotes comparisons indicating statistical significance compared to the control group, with *$p < 0.05$, **$p < 0.01$, and ***$p < 0.001$. "#" signifies comparisons indicating statistical significance compared to the LPS group, with #$p < 0.05$ and ##$p < 0.01$.

0.001). In the LPS + Mg group, BCL2 level was significantly higher compared to the control group ($p < 0.05$), while BAX and eIF2α levels were significantly lower ($p < 0.05$ and $p < 0.001$, respectively). Additionally, in the LPS + SLB group, eIF2α level was also found to be significantly higher compared to the control group ($p < 0.05$) (Fig. 11).

4. Discussion

The increased incidence of preterm labor and associated complications, such as PBI, due to infection-induced chorioamnionitis underscores the need for new treatment modalities for this public health issue. In light of the findings from our study, the most crucial conclusion is that the combined treatment of SLB and Mg has the potential to positively impact both maternal and neonatal health.

Inflammation occurring in placental tissue leads to increased permeability in placental blood vessels, allowing proinflammatory cytokines produced by inflammation to enter the fetal circulation (Goldstein et al., 2020). Histopathological analyses of placenta and fetal brain tissues revealed microhemorrhages and inflammatory cell infiltrations. Supporting these findings, immunohistochemical analyses indicating increased expressions of TNF-α, markers of acute inflammation, and Cas-3, a marker of apoptosis, suggest the presence of inflammation in the placenta, affecting vascular structures and culminating in apoptosis. The regression of these indicators in all treatment groups, with the most significant regression observed in the combined drug group, supports the hypothesis of the study. Previous studies by Suzuki et al. reported that Mg reduces inflammatory cytokine release in neonates (Suzuki-Kakisaka et al., 2013). Additionally, Anuncibay-Soto et al. demonstrated the anti-inflammatory effects of SLB in a global cerebral ischemia study, which aligns with the results of our study (Anuncibay-Soto et al., 2018). Although both molecules exhibit anti-inflammatory activity in various tissues and pathologies, their combined use has not been previously explored.

The activation of apoptotic cell death secondary to inflammation involves the role of TNF-α in stimulating Cas-3, particularly through the extrinsic pathway. Cellular damage can lead to apoptosis by disrupting functions such as protein folding and energy metabolism in the ER and mitochondria. Additionally, the stress occurring in the ER leads to an increase in the BAX/BCL2 ratio through the eIF2α pathway (Zhao et al., 2022). The impact of Mg on eIF2α has not been previously investigated in the literature. As evident in the study results, the elevation of eIF2α levels in response to LPS establishes ER stress as a significant mechanism of cellular damage. It is expected that SLB, which selectively exerts its effects on ER stress through eIF2α, would be more effective than Mg in a single application, consistent with the results. However, when used in combination, a significant difference was observed only compared to Mg.

qRT-PCR analysis measured BAX and BCL2 mRNA expressions in

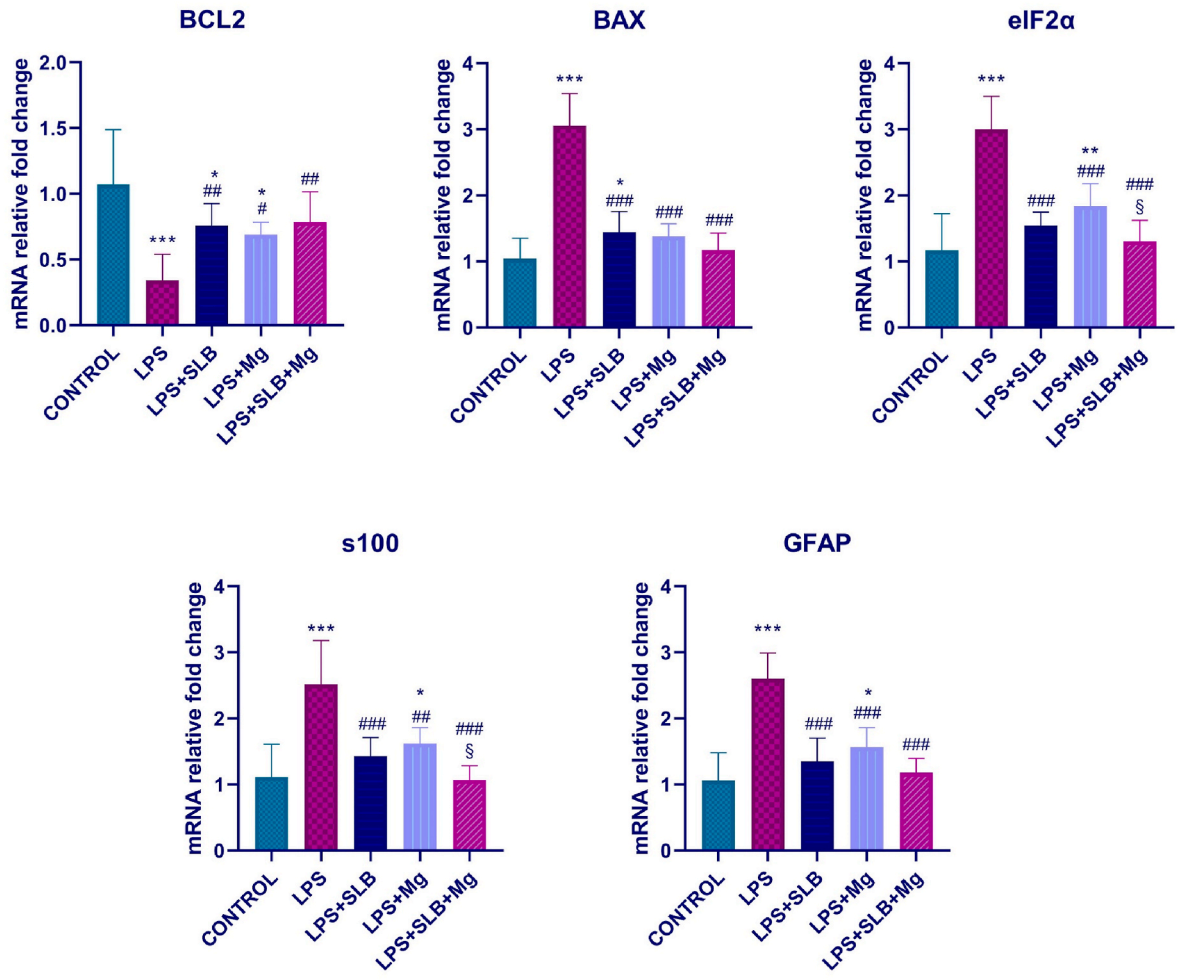

Fig. 10. The relative fold change graphs of genes in fetal brain tissues
Data were expressed as mean ± standard deviation. BCL2: B-cell lymphoma 2, BAX: BCL2-associated X protein, eIF2α: Eukaryotic Initiation Factor 2 Alpha, s100: S100 protein, GFAP: Glial fibrillary acidic protein, LPS: Lipopolysaccharide, SLB: Salubrinal, Mg: Magnesium. "*" denotes comparisons indicating statistical significance compared to the control group, with *$p < 0.05$, **$p < 0.01$, and ***$p < 0.001$. "#" signifies comparisons indicating statistical significance compared to the LPS group, with #$p < 0.05$, ##$p < 0.01$, and ###$p < 0.001$. "§" denotes comparisons indicating statistical significance compared to the LPS + Mg group, with §$p < 0.05$.

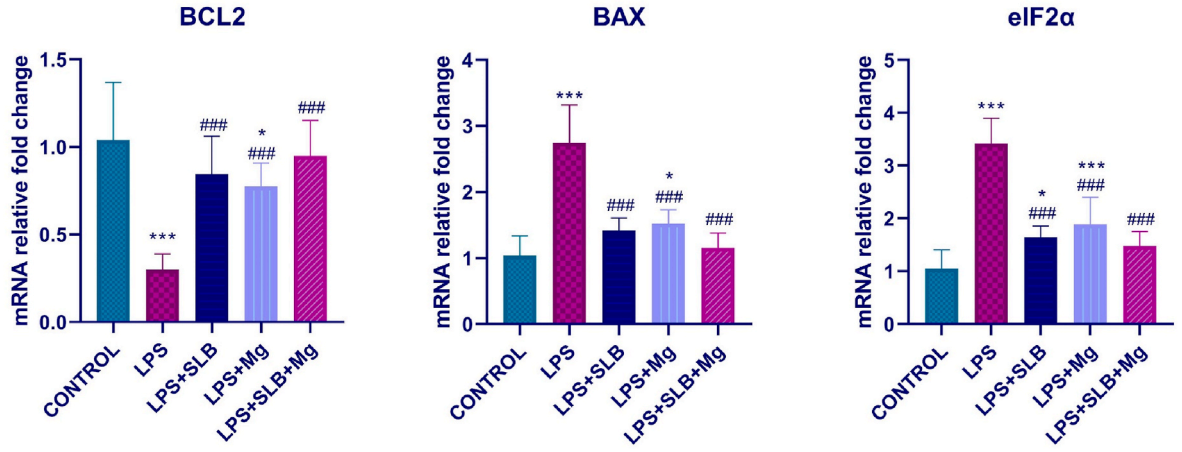

Fig. 11. The relative fold change graphs of genes in placental tissues
Data were expressed as mean ± standard deviation. BCL2: B-cell lymphoma 2, BAX: BCL2-associated X protein, eIF2α: Eukaryotic Initiation Factor 2 Alpha. "*" denotes comparisons indicating statistical significance compared to the control group, with *$p < 0.05$ and **$p < 0.001$. "###" signifies comparisons indicating statistical significance compared to the LPS group, with ###$p < 0.001$.

both tissues to assess apoptosis. In the LPS group, increased BAX and decreased BCL2 levels were reversed in all treatment groups. These results are consistent with the Cas-3 levels demonstrated immunohistochemically in our study. Chun-Lei et al. also showed SLB's inhibition of ER stress and prevention of apoptosis in a cell culture study (Chun-Lei et al., 2012). The decrease in the BAX/BCL2 ratio due to Mg has been demonstrated in the cerebral ischemia model conducted by Zhou et al. (2003). Although there were no significant advantages of BAX and BCL2 changes between the placenta and brain tissues in both the SLB and Mg groups compared to each other, their effects were enhanced in the combined application. Consequently, maintaining the BAX/BCL2 ratio in the placenta ensures placental integrity and perfusion, reducing disturbances in fetal circulation and preventing neuronal lesions due to anti-apoptotic effects in the brain.

Expression analyses of s100 and GFAP mRNA levels in fetal brains revealed improvement, especially with combined application. This observation, consistent with other analyses, supports the hypothesis. Also, positive effects of Mg on s100 and GFAP in a preeclampsia-like seizure model were demonstrated by Li et al. (2017). Although Wang et al. reported an increase in GFAP expression in traumatic brain injury with SLB, the effects of both agents on fetal brain development have not been assessed in any study (20).

Preventing oxidative stress and inflammation is crucial in inhibiting apoptotic cell death in case of progression of damage mechanisms. When examining oxidative stress parameters in the study results, the calculated OSI based on the oxidant/antioxidant ratio indicates the following: in placental tissue, the use of Mg and the combination; in fetal brain tissue, SLB, and combined application were found to be significantly effective. Consequently, combined use is advantageous due to the potentiation of preventive effects on oxidative stress and the superior effectiveness of agents in different tissues.

The increase in antioxidant enzyme synthesis in fetal brain tissues with SLB and combined application, but the absence of this effect in placental tissues, is insufficient evidence to establish that SLB directly enhances antioxidant enzyme synthesis. Additionally, the inability of Mg application to increase TAS levels in both tissues suggests that the effects of SLB and Mg may be attributed to the reduction of oxidative stress through mechanisms such as inflammation and ER stress, rather than direct antioxidant effects.

Limitations of the study include the absence of cognitive or behavioral tests for the fetal neurodevelopment of offsprings and the inability to observe the effects of inflammation in the chronic period. Additionally, the study did not demonstrate the dephosphorylated/phosphorylated eIF2α protein levels. These analyses, which could not be performed due to physical and economic constraints, will be completed in future studies.

5. Conclusion

In conclusion, the efficacy of the known anti-inflammatory agent Mg and the ER stress inhibitor SLB, individually and in combination, has been assessed in chorioamnionitis. The combination of these agents has proven superior due to both tissue-specific differences in efficacy and the cumulative tissue-protective effects. However, further studies with detailed clinical analyses are necessary to support the findings obtained for future validation.

Funding

Financial support for this research was provided by the Scientific Research Projects Coordination Unit of Suleyman Demirel University under project number TYL-2019-7406 and by TUBITAK under project number 222S711.

Disclosure statement

There are no financial or ethical conflicts of interest to be declared by the corresponding author and co-authors in connection with this study.

CRediT authorship contribution statement

Halil Asci: Writing – review & editing, Writing – original draft, Visualization, Validation, Supervision, Resources, Project administration, Methodology, Investigation, Funding acquisition, Data curation, Conceptualization. **Mehtap Savran:** Writing – review & editing, Writing – original draft, Supervision, Methodology, Investigation, Data curation, Conceptualization. **Muhammet Y. Tepebasi:** Writing – review & editing, Visualization, Validation, Formal analysis. **Ilter Ilhan:** Writing – review & editing, Validation, Formal analysis, Data curation. **Nasif F. Karakuyu:** Writing – review & editing, Resources, Investigation. **Orhan B. Imeci:** Writing – review & editing, Writing – original draft, Visualization, Validation, Project administration, Methodology, Investigation, Formal analysis, Data curation, Conceptualization. **Mehmet A. Sevuk:** Writing – review & editing, Writing – original draft, Visualization, Validation, Project administration, Methodology, Investigation, Data curation, Conceptualization. **Mekin Sezik:** Writing – review & editing, Supervision, Project administration, Conceptualization. **Ozlem Ozmen:** Writing – review & editing, Visualization, Validation, Supervision, Investigation, Formal analysis, Data curation.

Declaration of generative AI and AI-assisted technologies in the writing process

During the preparation of this work the authors used ChatGPT 3.5 in order to improve language and readability. After using this tool/service, the authors reviewed and edited the content as needed and takes full responsibility for the content of the publication.

Declaration of competing interest

The authors declare the following financial interests/personal relationships which may be considered as potential competing interests:

Halil Asci reports financial support was provided by Scientific and Technological Research Council of Turkey and Scientific Research Projects Coordination Unit of Suleyman Demirel University. If there are other authors, they declare that they have no known competing financial interests or personal relationships that could have appeared to influence the work reported in this paper.

Data availability

Data will be made available on request.

References

Anuncibay-Soto, B., Pérez-Rodriguez, D., Santos-Galdiano, M., Font-Belmonte, E., Ugidos, I.F., Gonzalez-Rodriguez, P., Regueiro-Purriños, M., Fernández-López, A., 2018. Salubrinal and robenacoxib treatment after global cerebral ischemia. Exploring the interactions between ER stress and inflammation. Biochem. Pharmacol. 151, 26–37. https://doi.org/10.1016/j.bcp.2018.02.029.

Beloosesky, R., Khatib, N., Ginsberg, Y., Anabosy, S., Shalom-Paz, E., Dahis, M., Ross, M. G., Weiner, Z., 2016. Maternal magnesium sulfate fetal neuroprotective effects to the fetus: inhibition of neuronal nitric oxide synthase and nuclear factor kappa-light-chain-enhancer of activated B cells activation in a rodent model. Am. J. Obstet. Gynecol. 215, 382.e1–382.e6. https://doi.org/10.1016/j.ajog.2016.03.032.

Bracchi-Ricard, V., Lambertsen, K.L., Ricard, J., Nathanson, L., Karmally, S., Johnstone, J., Ellman, D.G., Frydel, B., McTigue, D.M., Bethea, J.R., 2013. Inhibition of astroglial NF-κB enhances oligodendrogenesis following spinal cord injury. J. Neuroinflammation 10, 92. https://doi.org/10.1186/1742-2094-10-92.

Chun-Lei, L., Xin, L., Guo-Liang, H., Rui-Jun, L., Yun-Yun, H., Wu, Z., Song, L., Kun-Lun, H., Li-Li, W., 2012. Salubrinal protects against tunicamycin and hypoxia induced cardiomyocyte apoptosis via the PERK-eIF2α signaling pathwaySalubrinal protects against tunicamycin and hypoxia induced cardiomyocyte apoptosis via the

PERK-eIF2α signaling pathway. J. Geriatric Cardiology 9, 258–268. https://doi.org/10.3724/SP.J.1263.2012.02292.
Conti, N., Torricelli, M., Voltolini, C., Vannuccini, S., Clifton, V.L., Bloise, E., Petraglia, F., 2015. Term histologic chorioamnionitis: a heterogeneous condition. Eur. J. Obstet. Gynecol. Reprod. Biol. 188, 34–38. https://doi.org/10.1016/J.EJOGRB.2015.02.034.
Deselms, H., Maggio, N., Rubovitch, V., Chapman, J., Schreiber, S., Tweedie, D., Kim, D. S., Greig, N.H., Pick, C.G., 2016. Novel pharmaceutical treatments for minimal traumatic brain injury and evaluation of animal models and methodologies supporting their development. J. Neurosci. Methods 272, 69–76. https://doi.org/10.1016/j.jneumeth.2016.02.002.
Eklind, S., Mallard, C., Leverin, A.L., Gilland, E., Blomgren, K., Mattsby-Baltzer, I., Hagberg, H., 2001. Bacterial endotoxin sensitizes the immature brain to hypoxic–ischaemic injury. Eur. J. Neurosci. 13, 1101–1106. https://doi.org/10.1046/J.0953-816X.2001.01474.X.
Goldstein, J.A., Gallagher, K., Beck, C., Kumar, R., Gernand, A.D., 2020. Maternal-fetal inflammation in the placenta and the developmental origins of health and disease. Front. Immunol. 11, 531543 https://doi.org/10.3389/fimmu.2020.531543.
Heine, R.P., Puopolo, K.M., Beigi, R., Silverman, N.S., El-Sayed, Y.Y., 2017. Committee opinion No. 712: intrapartum management of intraamniotic infection. Obstet. Gynecol. 130, E95–E101. https://doi.org/10.1097/AOG.0000000000002236.
Huang, X., Chen, Y., Zhang, H., Ma, Q., Zhang, Y., Xu, H., 2012. Salubrinal attenuates β-amyloid-induced neuronal death and microglial activation by inhibition of the NF-κB pathway. Neurobiol. Aging 33. https://doi.org/10.1016/j.neurobiolaging.2011.10.007, 1007.e9–17.
Khatib, N., Ginsberg, Y., Shalom-Paz, E., Dabaja, H., Gutzeit, O., Zmora, O., Millo, Z., Ross, M.G., Weiner, Z., Beloosesky, R., 2020. Fetal neuroprotective mechanism of maternal magnesium sulfate for late gestation inflammation: in a rodent model. J. Matern. Fetal Neonatal Med. 33, 3732–3739. https://doi.org/10.1080/14767058.2019.1583735.
Larroque, B., Ancel, P.Y., Marret, S., Marchand, L., André, M., Arnaud, C., Pierrat, V., Rozé, J.C., Messer, J., Thiriez, G., Burguet, A., Picaud, J.C., Bréart, G., Kaminski, M., 2008. Neurodevelopmental disabilities and special care of 5-year-old children born before 33 weeks of gestation (the EPIPAGE study): a longitudinal cohort study. Lancet 371, 813–820. https://doi.org/10.1016/S0140-6736(08)60380-3.
Li, X., Han, X., Yang, J., Bao, J., Di, X., Zhang, G., Liu, H., 2017. Magnesium sulfate provides neuroprotection in eclampsia-like seizure model by ameliorating neuroinflammation and brain edema. Mol. Neurobiol. 54, 7938–7948. https://doi.org/10.1007/s12035-016-0278-4.
Matsuoka, M., Komoike, Y., 2015. Experimental evidence shows salubrinal, an eIF2α dephosphorylation inhibitor, reduces xenotoxicant-induced cellular damage. Int. J. Mol. Sci. 16, 16275–16287. https://doi.org/10.3390/ijms160716275.
Novak, C.M., Ozen, M., Burd, I., 2018. Perinatal brain injury: mechanisms, prevention, and outcomes. Clin. Perinatol. 45, 357–375. https://doi.org/10.1016/J.CLP.2018.01.015.
Oakes, S.A., Papa, F.R., 2015. The role of endoplasmic reticulum stress in human pathology. Annu. Rev. Pathol. 10, 173–194. https://doi.org/10.1146/ANNUREV-PATHOL-012513-104649.
Ohyama, M., Itani, Y., Yamanaka, M., Goto, A., Kato, K., Ijiri, R., Tanaka, Y., 2002. Re-evaluation of chorioamnionitis and funisitis with a special reference to subacute chorioamnionitis. Hum. Pathol. 33, 183–190. https://doi.org/10.1053/hupa.2002.31291.
Özden, E.S., Aşcı, H., Büyükbayram, H.İ., Sevük, M.A., İmeci, O.B., Doğan, H.K., Özmen, Ö., 2023. Dexpanthenol protects against lipopolysaccharide-induced acute kidney injury by restoring aquaporin-2 levels via regulation of the silent information regulator 1 signaling pathway. Korean J Anesthesiol 76, 501–509. https://doi.org/10.4097/KJA.23207.
Perkins, R.P., Butler, C., Zhou, S. mei, Skipper, B.J., 1988. Histologic chorioamnionitis in pregnancies of various gestational ages. II: implications in preterm labor. Am. J. Perinatol. 5, 300–303. https://doi.org/10.1055/S-2007-999710.
Ron, D., Walter, P., 2007. Signal integration in the endoplasmic reticulum unfolded protein response. Nat. Rev. Mol. Cell Biol. 8, 519–529. https://doi.org/10.1038/nrm2199.
Roth, T.L., Nayak, D., Atanasijevic, T., Koretsky, A.P., Latour, L.L., McGavern, D.B., 2014. Transcranial amelioration of inflammation and cell death after brain injury. Nature 505, 223–228. https://doi.org/10.1038/nature12808.
Rubovitch, V., Barak, S., Rachmany, L., Goldstein, R.B., Zilberstein, Y., Pick, C.G., 2015. The neuroprotective effect of salubrinal in a mouse model of traumatic brain injury. NeuroMolecular Med. 17, 58–70. https://doi.org/10.1007/s12017-015-8340-3.
Suzuki-Kakisaka, H., Sugimoto, J., Tetarbe, M., Romani, A.M., Ramirez Kitchen, C.M., Bernstein, H.B., 2013. Magnesium sulfate increases intracellular magnesium reducing inflammatory cytokine release in neonates. Am. J. Reprod. Immunol. 70, 213–220. https://doi.org/10.1111/aji.12118.
Tan, H.-P., Guo, Q., Hua, G., Chen, J.-X., Liang, J.-C., 2018. Inhibition of endoplasmic reticulum stress alleviates secondary injury after traumatic brain injury. Neural Regen Res 13, 827–836. https://doi.org/10.4103/1673-5374.232477.
Wang, Z., Gao, C., Chen, W., Gao, Y., Wang, H., Meng, Y., Luo, C., Zhang, M., Chen, G., Chen, X., Wang, T., Tao, L., 2019. Salubrinal offers neuroprotection through suppressing endoplasmic reticulum stress, autophagy and apoptosis in a mouse traumatic brain injury model. Neurobiol. Learn. Mem. 161, 12–25. https://doi.org/10.1016/j.nlm.2019.03.002.
Yavuz, A., Sezik, M., Ozmen, O., Asci, H., 2017. Fingolimod against endotoxin-induced fetal brain injury in a rat model. J. Obstet. Gynaecol. Res. 43, 1708–1713. https://doi.org/10.1111/jog.13444.
Zhang, K., Kaufman, R.J., 2004. Signaling the unfolded protein response from the endoplasmic reticulum. J. Biol. Chem. 279, 25935–25938. https://doi.org/10.1074/JBC.R400008200.
Zhao, Y., Ding, M., Yang, N., Huang, Y., Sun, C., Shi, W., 2022. Zinc accumulation aggravates cerebral ischemia/reperfusion injury through inducing endoplasmic reticulum stress. Neurochem. Res. 47, 1419–1428. https://doi.org/10.1007/s11064-022-03536-w.
Zhou, H., Ma, Y., Zhou, Y., Liu, Z., Wang, K., Chen, G., 2003. Effects of magnesium sulfate on neuron apoptosis and expression of caspase-3, bax and bcl-2 after cerebral ischemia-reperfusion injury. Chin. Med. J. 116, 1532–1534.